

Gamma-Ray Transitions between the Low-Lying Levels of $F^{18}\dagger$

E. K. WARBURTON, J. W. OLNES, AND A. R. POLETTI

Brookhaven National Laboratory, Upton, New York

(Received 25 October 1966)

Gamma-ray decay modes of the F^{18} levels below an excitation energy of 4 MeV have been investigated through the $O^{16}(He^3, p\gamma)F^{18}$ reaction using a 30-cc lithium-drifted germanium, Ge(Li), detector. Gamma-ray spectra were recorded at 90° , 7° , and 173° to the He^3 beam using a thick quartz target and He^3 bombarding energies of 3.45 and 6.0 MeV. Ge(Li)-NaI(Tl) coincidence spectra were also recorded at $E_{He^3}=3.2$ MeV. Sharper upper limits than obtained previously were set on the relative intensities of many unobserved transitions. A previously unreported transition from the $J=1$ 3.13-MeV level to the $J^\pi=0^-$ 1.08-MeV level was observed with a branching ratio of $(27\pm 4)\%$. The mean lifetime of the 3.13-MeV level was inferred from a Doppler-shift measurement to be $(0.37_{-0.10}^{+0.18})\times 10^{-12}$ sec. It is conjectured that the 3.13-MeV level is the lowest $J^\pi=1^-$ level belonging predominantly to the $p^{-1}(2s, 1d)^3$ configuration.

I. INTRODUCTION

THE principal gamma-ray decay modes of the nuclear energy levels below an excitation energy of 4 MeV in F^{18} have been well-established, mainly by particle-gamma coincidence measurements using the $O^{16}(He^3, p)F^{18}$ reaction.¹⁻⁷ These experiments were performed with NaI(Tl) gamma-ray detectors which have an energy resolution which is inadequate for separating all of the possible gamma-ray transitions from the levels above the fourth. Thus it is conceivable that some relatively strong but unresolved transitions have been missed in these studies. For the same reasons, it has been impossible in many cases to set stringent upper limits on the relative intensities of all the non-observed transitions.

The measurements described in this report were therefore carried out to search for weak gamma-ray transitions from the F^{18} states below 4-MeV excitation and also to supplement a previous investigation⁶ of the lifetimes of these levels by means of the Doppler-shift attenuation method. The present measurements employed a 30-cc Ge(Li) crystal to detect gamma rays from the He^3 bombardment of O^{16} ; both singles spectra and gamma-gamma coincidence spectra were recorded, the latter using a 3×3 -in. NaI(Tl) crystal in time coincidence with the Ge(Li) detector.

II. EXPERIMENTAL PROCEDURES AND RESULTS

A. Gamma-Ray Energy Measurements

The target for all of the measurements was a quartz (SiO_2) plate infinitely thick to the incident He^3 beam. Gamma-ray spectra produced by bombardment of the quartz with a 3.45-MeV He^3 beam were measured with the 30-cc Ge(Li) detector which was placed variously at 90° , 7° , and 173° to the incident beam. Pulse-height spectra from the detector were recorded using a 4096-channel pulse-height analyzer which was provided with digital pulse-stabilization. These spectra included the energy region from 400 to 4380 keV and had a dispersion of 0.973 keV/channel. The energy calibration was internal, consisting of annihilation radiation, gamma rays⁸ of 5104.87 ± 0.18 and 2792.68 ± 0.15 keV from the long-lived 5.1-MeV level of N^{14} populated by the $C^{12}(He^3, p)N^{14}$ reaction (arising from carbon contamination of the target and beam defining aperture), and the O^{15} (5240.53 \pm 0.52)-keV line⁸ originating from the 5.24-MeV level in O^{15} populated by the $O^{16}(He^3, \alpha)O^{15}$ reaction. The long life of the levels from which these latter three gamma rays originated ensured that the gamma rays were neither Doppler shifted nor broadened. The resolution (full width at half-maximum) achieved in these spectra varied with energy from 7 keV for the 511-keV annihilation radiation to 17.6 keV for the two-escape peak of the O^{15} 5241-keV line.

Gamma-ray energies were extracted from the 90° spectrum. The procedures used have been described previously.⁹ The results are given in Table I which includes the measured energies, the associated uncertainties, and the assignment of the gamma rays to transitions in F^{18} . No attempt was made to determine the energies of unresolved gamma-ray lines. The identification of the lines is based on the known¹⁻⁷ decay schemes, on the coincidence measurements described in this report, and on a supplementary spectrum

[†] Work performed under the auspices of the U. S. Atomic Energy Commission.

¹ J. A. Kuehner, E. Almqvist, and D. A. Bromley, *Phys. Rev.* **122**, 908 (1961).

² A. R. Poletti and E. K. Warburton, *Phys. Rev.* **137**, B595 (1965).

³ C. Chasman, K. W. Jones, R. A. Ristinen, and E. K. Warburton, *Phys. Rev.* **137**, B1445 (1965).

⁴ J. W. Olness and E. K. Warburton, *Bull. Am. Phys. Soc.* **11**, 405 (1966); *Phys. Rev.* (to be published).

⁵ P. R. Chagnon, *Nucl. Phys.* **78**, 193 (1966); **81**, 433 (1966).

⁶ J. W. Olness and E. K. Warburton, *Phys. Rev.* **151**, 792 (1966).

⁷ S. Gorodetzky, R. M. Freeman, A. Gallmann, F. Haas, and B. Heusch, this issue, *Phys. Rev.* **155**, 1119 (1967).

⁸ C. Chasman, K. W. Jones, R. A. Ristinen, and D. E. Alburger (to be published).

⁹ H. H. Williams, E. K. Warburton, K. W. Jones, and J. W. Olness, *Phys. Rev.* **144**, 801 (1966).

recorded at 90° with an incident He^3 beam of 6 MeV. For some of the gamma rays, both full-energy and two-escape peaks were observed, while for two of the gamma rays, one-escape peaks were also observed. The interpretation of these spectra was facilitated by curves for the relative efficiencies for detection of the full-energy, one-escape, and two-escape peaks as determined for a 25-cc Ge(Li) counter.¹⁰ The uncertainties assigned in Table I include our estimates of possible Doppler effects.^{3,6}

The gamma-ray energies of Table I were used to obtain the F^{18} excitation energies listed in the second column of Table II. The recoil effect was taken account of in the conversion from gamma-ray energy to excitation energy. The results of Chasman *et al.*³ listed in the third column are from a similar measurement; while other previous results are listed in column 4.

A comparison of the various results listed in Table II indicates that the tentative results reported by Chasman *et al.*³ for levels 4 and 10 should be discounted while for the remaining transitions their energies are systematically higher than the present ones. The adopted values for the F^{18} excitation energies, listed in the last column of Table II, are not weighted averages (with the exception of the first three levels) but are based mainly on the present work including also some results from the coincidence spectra to be considered in Sec. IIC. Level 12 is assigned an uncertainty of 5 keV instead of the original 10 keV because of the excellent agreement between columns 2 and 4 for the excitation energies of levels 11 and 13.

B. Gamma-Ray Doppler-Shift Measurements

The excitation energies listed in Table II were quite useful in predicting the expected positions of previously unobserved transitions. The 90° spectra were recorded for this reason and also to search for or set intensity limits on previously unobserved transitions. The 7° and 173° spectra were recorded with the specific

TABLE I. Gamma rays from $O^{16}(He^3, p)F^{18}$.

E_γ (keV)	Assignment
658.75 \pm 0.7	1.70 \rightarrow 1.04
777.9 \pm 1	3.84 \rightarrow 3.06
936.9 \pm 1	0.94 \rightarrow 0
1020.4 \pm 1	2.10 \rightarrow 1.08
1041.3 \pm 1.5	1.04 \rightarrow 0
1080.2 \pm 1	1.08 \rightarrow 0
1163.2 \pm 1	2.10 \rightarrow 0.94
1586.5 \pm 1.5	2.52 \rightarrow 0.94
1657.5 \pm 3	3.36 \rightarrow 1.70
1700.3 \pm 1.5	1.70 \rightarrow 0
2053.8 \pm 2	3.13 \rightarrow 1.08
2123.2 \pm 2	3.06 \rightarrow 0.94
2523.3 \pm 2.5	2.52 \rightarrow 0
2682.9 \pm 3	3.72 \rightarrow 1.04
3060.2 \pm 3	3.06 \rightarrow 0
3133.3 \pm 3	3.13 \rightarrow 0

¹⁰ We wish to thank T. K. Alexander for making these curves available to us.

TABLE II. Excitation energies of the low-lying levels of F^{18} .

Level	Present work (keV)	Chasman <i>et al.</i> ^a (keV)	Previous work ^b (keV)	Adopted values (keV)
1	937.0 \pm 1	937.4 \pm 1.5	940	937.1 \pm 1
2	1041.3 \pm 1.5	1044.6 \pm 1.5	1041.7 \pm 0.6 ^c	1041.7 \pm 0.6
3	1080.3 \pm 1	1081.7 \pm 1.5	1085	1080.7 \pm 1
4	...	(1119.7 \pm 2)	1131.0 \pm 1.5 ^d	1131.0 \pm 1.5
5	1700.3 \pm 1.5	1703.5 \pm 2	1700	1700.5 \pm 0.9
6	2100.5 \pm 1.5	2102.6 \pm 2	2104	2100.8 \pm 1.5
7	2523.5 \pm 1.5	2529.7 \pm 2	2525	2523.5 \pm 1.5
8	3060.3 \pm 3	...	3063	3060.3 \pm 3
9	3133.9 \pm 3	...	3133	3133.9 \pm 3
10	3358.1 \pm 3	(3350.5 \pm 3)	3354	3358.1 \pm 3
11	3724.8 \pm 3	...	3725	3724.8 \pm 3
12	3790	3790 \pm 5
13	3838.5 \pm 3.5	...	3839	3838.5 \pm 3.5

^a C. Chasman, K. W. Jones, R. A. Ristinen, and E. K. Warburton, Phys. Rev. **137**, B1445 (1965).

^b Unless otherwise noted these values are from F. Ajzenberg-Selove and T. Lauritsen [Nucl. Phys. **11**, 1 (1959)] and have uncertainties of ± 10 keV.

^c A. E. Blaugrund, D. H. Youngblood, G. C. Morrison, and R. E. Segel, Phys. Rev. (to be published).

^d T. K. Alexander, K. W. Allen, and D. C. Healy, Phys. Letters **20**, 402 (1966).

purpose of obtaining information on the Doppler shifts of the $3.13 \rightarrow 0$ and $3.72 \rightarrow 1.04$ transitions. The Doppler shifts of at least one of the transitions originating from each of the other energy levels of column 1, Table II, had been measured in a previous study.⁶ The present Doppler-shift measurements were performed using the same apparatus as was used previously⁶ with the exception that a 30-cc Ge(Li) detector replaced the earlier 3.5-cc detector. One consequence of this was that the full energy peaks of the $3.06 \rightarrow 0$, $3.13 \rightarrow 0$, and $3.72 \rightarrow 1.04$ transitions were readily apparent in the present work. With the 3.5-cc detector these peaks were lost in the background, and the lifetime of the 3.06-MeV level was investigated via the $3.06 \rightarrow 0.94$ transition, while the lifetimes of the 3.13- and 3.72-MeV levels were not investigated.

The Doppler shifts of all the gamma-ray peaks with energies between 2.5 and 3.4 MeV were extracted from the 7° and 173° spectra using computer techniques.⁶ The portions of these spectra showing the full-energy peaks of the $3.06 \rightarrow 0$ and $3.13 \rightarrow 0$ transitions are plotted in Fig. 1. The experimental Doppler shifts are

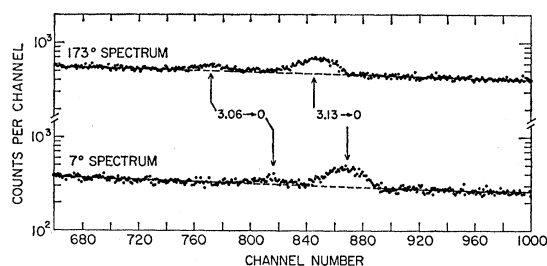


Fig. 1. Partial spectra of gamma rays from $O^{16} + 3.45$ -MeV He^3 detected by a 30-cc Ge(Li) crystal. The full-energy peaks of the $3.06 \rightarrow 0$ and $3.13 \rightarrow 0$ transitions are indicated. The spectra were recorded with a dispersion of 1.081 keV/channel and were measured at 7° to the He^3 beam (bottom) and 173° to the He^3 beam (top).

TABLE III. Summary of Doppler-shift results for some transitions in F^{18} .

F^{18} transition	$\langle \Delta E_\gamma \rangle_{\text{expt}}$ (keV)			$\langle \Delta E_\gamma \rangle_{\text{calc}}$ (keV)	F'^b	From F'	τ_m^c (psec) Other results	Average
	Present	Previous ^a	Average					
2.52 \rightarrow 0	13.0 \pm 0.7	13.3 \pm 0.7	13.1 \pm 0.5	35.9 \pm 6.0	0.37 \pm 0.06	0.63 $_{-0.14}^{+0.18}$	{1.1 \pm 0.2 ^d 0.69 \pm 0.14 ^e }	0.80 \pm 0.14
3.06 \rightarrow 0	43.0 \pm 2.3	45.0 \pm 2.3	44.0 \pm 2	43.6 \pm 6.3	1.01 \pm 0.15	<0.20	...	<0.20
3.13 \rightarrow 0	22.6 \pm 2	...	22.6 \pm 2	44.7 \pm 6.4	0.51 \pm 0.09	0.37 $_{-0.10}^{+0.15}$...	0.37 $_{-0.10}^{+0.15}$
3.72 \rightarrow 1.04	45.7 \pm 3	...	45.7 \pm 3	38.2 \pm 4.3	1.20 \pm 0.14	<0.08	...	<0.08
3.35 \rightarrow 0	19.2 \pm 3	19.7 \pm 3.2	19.4 \pm 2.5	47.7 \pm 6.3	0.41 \pm 0.08	0.55 $_{-0.15}^{+0.20}$	0.45 $_{-0.10}^{+0.15e}$	0.50 $_{-0.25}^{+0.20}$
3.84 \rightarrow 0	56.0 \pm 2	59.7 \pm 2	57.8 \pm 1.4	54.5 \pm 5.7	1.06 \pm 0.12	<0.1	...	<0.1

^a Reference 6.

^b F' is the ratio $\langle \Delta E_\gamma \rangle_{\text{expt}} / \langle \Delta E_\gamma \rangle_{\text{calc}}$ where $\langle \Delta E_\gamma \rangle_{\text{calc}}$ is the maximum expected energy shift computed from the known reaction kinematics.

^c The values quoted are the mean lifetimes (or their limits) of the initial states listed in column 1.

^d A. E. Litherland, M. J. L. Yates, B. M. Hinds, and D. Eccleshall, Nucl. Phys. **44**, 220 (1963).

^e Revised values obtained for the line-shift analysis of Ref. 6.

listed in Table III together with those measured previously⁶ under identical geometrical and kinematical conditions. It is seen that the agreement between the two sets of measurements is excellent, and we therefore use the indicated average values to compute the attenuation factors F' and subsequently the mean lives τ_m . The average values listed in Table III for τ_m were obtained by combining the present results with those of other investigations as indicated.

The procedures used to obtain the lifetimes τ_m from the experimental values of F' are described in detail by Olness and Warburton.⁶ We note here that the inclusion of recent stopping power data results in a curve of dE/dx versus E slightly different from that used previously,⁶ as characterized by a revised electronic-stopping time $\alpha = (0.52 \pm 0.07) \times 10^{-12}$ sec and a nuclear-stopping parameter $\gamma_i^2 = (11_{-5}^{+8})$. The data of Ref. 6 have therefore been reexamined using the above values of γ_i^2 and α , together with an improved method of analysis (computer based), from which we conclude that the mean-life times quoted previously⁶ for the 1.70- and 2.10-MeV levels should be revised to yield the values (1.0 \pm 0.3) psec and (5.0 $_{-2}^{+3}$) psec respectively. We now average these values with the prior information given in Ref. 6 to obtain $\tau_m = (1.1 \pm 0.3)$ psec for the F^{18} 1.70-MeV level and $\tau_m = (5.1_{-2}^{+3})$ psec for the 2.10-MeV level. These results supersede those given previously.⁶

C. Gamma-Gamma Coincidence Measurements

Various Ge(Li) spectra of F^{18} gamma rays were recorded in coincidence with gamma-ray pulses from a 3 \times 3-in. NaI(Tl) crystal placed at 90 $^\circ$ to the beam and 2 cm from the target. The Ge(Li) detector was placed at 4 cm from the target at either 90 $^\circ$ or 0 $^\circ$ to the beam. The quartz target was bombarded by 3.2-MeV He³ ions. Pulses from both detectors were amplified and shaped by ORTEC Model 220 linear pulse systems which were also used to form coincidences between the detectors. The resolving time was \sim 30 nsec and the real/random ratio was \sim 20:1.

Four 1024-channel Ge(Li) spectra were recorded

simultaneously using the model 245 "spectrum sorter" facility of the TMC 16384-channel analyzer. This facility allows for the simultaneous recording of up to eight 1024-channel spectra in coincidence with the same number of digital gates, or "windows," set on the pulse-height spectrum of the other detector.

The first group of 4 Ge(Li) spectra were recorded at 90 $^\circ$ to the beam for a total elapsed time of 40 h with a beam intensity of 20 nA. These spectra covered the gamma-ray energy region from 850 to 2340 keV, and were measured in coincidence with four separate windows set on the NaI(Tl) spectrum. The windows were centered on (1) the full-energy-loss peak of the 1.70 \rightarrow 1.04 gamma ray, (2) the full-energy-loss peak of the 0.94 \rightarrow 0 gamma ray, (3) the gamma-ray energy region from 1.0–1.1 MeV, and (4) the energy region from 1.3–1.4 MeV. The (1.0–1.1)-MeV window was set to include the full-energy-loss peaks of the 1.04 \rightarrow 0, 1.08 \rightarrow 0, and 2.10 \rightarrow 1.08 transitions, and also a portion of that due to the 2.10 \rightarrow 0.94 transition. The window from 1.3–1.4 MeV contained no observable gamma peaks so that the Ge(Li) spectrum in coincidence with it served as an estimate of the background for spectrum (3). Portions of these 4 Ge(Li) spectra are displayed in Figs. 2 and 3.

Figure 2 displays the data and analysis used to set an upper limit ($<0.8\%$) on the 2.10 \rightarrow 1.04 branching ratio. The datum points are a portion of the spectrum measured in coincidence with the 1-MeV complex of gamma peaks. Gamma-ray peaks corresponding to the 2.10 \rightarrow 1.08, 1.08 \rightarrow 0, and 1.04 \rightarrow 0 transitions are easily identified. The 1.04- and 1.08-MeV peaks were also observed in the "background" spectrum and it was determined that the relative intensities of the 1.04-MeV peak in the two spectra were consistent with those expected assuming that the 1.04-MeV gamma rays arose from coincidences with the Compton distributions of higher-energy gamma rays (which will be identified below). Thus, Fig. 2 provides no evidence for coincidences between the gamma rays from the 1.04 \rightarrow 0 transition and other gamma rays with energies of \sim 1 MeV. In particular there is no evidence for a 2.10 \rightarrow 1.04 transition. In order to set as sharp an upper limit as

possible on the relative branching ratio of this transition a computer-implemented fit was made to the spectra of Fig. 2 as follows. An exponential background was assumed under the three gamma-ray peaks of Fig. 2 and this background (the solid straight line in Fig. 2) was determined by a least-squares fit to pulse-height regions just above and below the region illustrated in Fig. 2. A least-squares fit was then made assuming three peaks superimposed on this exponential background. The peak response function used consisted of a Gaussian plus an exponential tail. The "tail" parameters were determined as a function of energy by least-squares fits to the isolated gamma-ray peaks corresponding to the $0.94 \rightarrow 0$ and $2.10 \rightarrow 0.94$ transitions and also to the $2.10 \rightarrow 1.08$ transition (Fig. 2). These parameters were fixed relative to the intensity of the Gaussian component of the peak in the subsequent least-squares fit. The solid curve through the datum points in Fig. 2 is one of several fits made in somewhat different ways. In addition a fit was made to the spectrum generated by subtracting the two spectra illustrated in Fig. 2. All gave excellent fits to the data. From this analysis we set a limit of $<0.8\%$ for the $2.10 \rightarrow 1.04$ branching ratio. The shape of the spectrum expected if the branching ratio of the 1059.1-keV ($2.10 \rightarrow 1.04$) transition were 1% is illustrated by the dotted curve of Fig. 2.

In Fig. 3 are shown the upper portions of two of the four spectra just discussed. The $3.06 \rightarrow 0.94$ and $3.13 \rightarrow 1.04$ peaks are evident as was expected. From these spectra upper limits were set on the branching

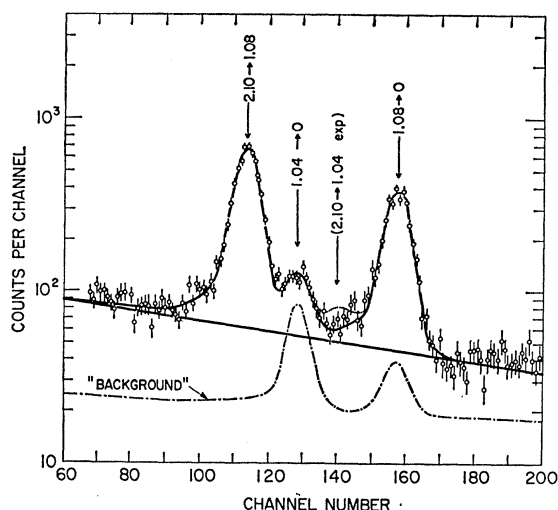


FIG. 2. Partial spectra of F^{18} gamma rays from $O^{16}+3.2$ -MeV He^3 ions recorded by a 30-cc Ge(Li) detector. The datum points show a portion of the spectrum recorded in coincidence with a gate set on the pulse-height region from 1.0 to 1.1 MeV as viewed by a 3×3 -in. NaI(Tl) crystal. The full-energy peaks are labeled by the energies of the initial and final states in MeV. The solid lines represent computer fits to this data as explained in the text. The dot-dashed line indicated as "BACKGROUND" represents the spectrum in coincidence with the region 1.3–1.4 MeV in the NaI(Tl) spectrum. The dispersion is 1.44 keV/channel.

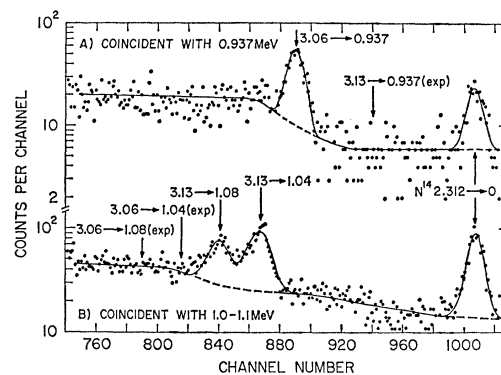


FIG. 3. Partial spectra of F^{18} gamma rays from $O^{16}+3.2$ -MeV He^3 ions recorded by a 30-cc Ge(Li) detector in coincidence with pulses from a NaI(Tl) detector. The N^{14} line is from $C^{12}+He^3$ due to a carbon contaminant. These partial spectra were part of the same group of four 1024-channel spectra as those of Fig. 2.

ratios of the $3.13 \rightarrow 0.94$, $3.06 \rightarrow 1.04$, and $3.06 \rightarrow 1.08$ transitions. The $3.13 \rightarrow 1.08$ transition had not been observed previously. As a check on the identification of this transition the Ge(Li) detector was placed at 0° to the beam and the experiment was repeated with all other conditions unchanged. The purpose of this was to check that the percentage Doppler shifts of the $3.13 \rightarrow 1.04$ and $3.13 \rightarrow 1.08$ transitions were the same. If our identification of these two lines is correct this must be so. This was done by determining the energy separation of the two peaks at 0° and 90° to the beam. These separations, determined by least-squares fits to the data, were found to be in agreement with each other and had an average value of 37.5 ± 1.1 keV as compared to 39.0 ± 1.1 keV (Table II) for the energy separation of the 1.04- and 1.08-MeV levels.

Two further sets of four 1024-channel coincidence spectra were recorded, both with the Ge(Li) detector at 90° to the beam. One was taken with identical conditions to the 90° set previously described with the exception that the gamma-ray energy region from 527 to 1813 keV was displayed. The other set was taken in coincidence with "windows" centered on approximately 1.5-, 2.1-, 2.5-, and 3.1-MeV regions of the NaI(Tl) spectrum. Partial spectra from 3 of these latter spectra are shown in Fig. 4. As in Fig. 3, the solid curves illustrate least-squares fits to the data in the region of peaks (with the assumed background shown by the dashed curves) and an arbitrary interpolation of these curves in the region between peaks. Curve B of Fig. 4 shows the 1.04- and 1.08-MeV peaks which are expected to be in coincidence with the 2.09- and 2.05-MeV photopeaks (Fig. 3) of the $3.13 \rightarrow 1.04$ and $3.13 \rightarrow 1.08$ transitions, respectively. Their appearance here provides supporting evidence for the conclusion (above) that the 3.13-MeV level branches to both the 1.04- and 1.08-MeV levels. The presence of the 0.94-MeV peak in B results from coincidences with the $3.06 \rightarrow 0.94$ gamma rays, while its presence in A results also from the $2.52 \rightarrow 0.94 \rightarrow 0$ cascade transition. Also seen in A are peaks of 0.66-

and 0.82-MeV from the $3.36 \rightarrow 1.70 \rightarrow 1.04$ and $2.52 \rightarrow 1.70 \rightarrow 0$ cascade transitions, respectively. We note that peaks which appear strongly in B must also appear in A due to coincidences with the Compton

TABLE IV. Gamma-ray branching ratios for the low-lying levels of F^{18} .

Level No.	E_i (MeV)	E_f (MeV)	E_γ (keV)	Branching ratios (%)		
				Previous ^a	Present ^b	Adopted
5	1.701	0	1700.5	31 ± 3	(31)	31 ± 3
		0.937	763.4	<10	<1	<1
		1.041	658.8	69 ± 3	(69)	69 ± 3
		1.081	619.8	<15	<3.5	<3.5
		1.131	569.5	<10	<3	<3
6	2.101	0	2100.8	36 ± 2	(36)	36 ± 2
		0.937	1163.7	31 ± 2	(31)	31 ± 2
		1.041	1059.1	<3	<0.8	<0.8
		1.081	1020.1	33 ± 2	(33)	33 ± 2
		1.131	969.8	<3	<2	<2
		1.701	400.3	<8	<4	<4
7	2.524	0	2523.5	74 ± 4	(74)	74 ± 4
		0.937	1586.4	22 ± 2	(22)	22 ± 2
		1.041	1481.8	<4	<0.5	<0.5
		1.081	1442.8	<4	<0.5	<0.5
		1.131	1392.5	<8	<4	<4
		1.701	823.0	4 ± 1.5	5 ± 2	4 ± 1.5
8	3.060	0	3060.3	25 ± 2	(25)	25 ± 2
		0.937	2123.2	75 ± 2	(75)	75 ± 2
		1.041	2018.6	<6	<6	<6
		1.081	1979.5	<8	<8	<8
		1.131	1929.3	<5	<14	<5
		1.701	1359.8	<5	<8	<5
		2.101	959.5	<15	<5	<5
		2.524	536.8	<10	<5	<5
		0	3133.9	32 ± 2	(32)	32 ± 2
		0.937	2196.8	...	<2	<2
9	3.134	1.041	2092.2	68 ± 2^c	41 ± 4	41 ± 4
		1.081	2053.2	...	27 ± 4	27 ± 4
		1.131	2003.4	<10	<8	<8
		1.701	1432.9	<4	<6	<4
		2.101	1033.1	<10	<6	<6
		2.524	610.4	<8	<1	<1
		0	3358.1	54 ± 5	(54)	53 ± 5
		0.937	2421.0	5 ± 3	7 ± 3	6 ± 3
		1.041	2316.4	<15	<5	<5
		1.081	2277.4	<10	<5	<5
10	3.358	1.131	2227.1	<10	<25	<10
		1.701	1657.6	35 ± 3	(35)	35 ± 3
		2.101	1257.3	6 ± 3	<20	6 ± 3
		2.524	834.6	<3	<25	<3
		0	3724.8	7 ± 2	16 ± 8	8 ± 2
		0.937	2787.7	<7	<6	<6
		1.041	2683.1	93 ± 2	(92)	92 ± 2
		1.081	2644.1	<20	<15	<15
		1.131	2593.8	<10	<15	<10
		1.701	2024.3	<6	...	<6
11	3.724	2.101	1624.0	<10	<30	<10
		2.524	1201.3	<3	<15	<3
		3.060	644.5	<5	<10	<5
		3.134	590.9	<3	<5	<3
		3.358	366.7	<4	<14	<4
		0	3790.0	<15	<20	<15
		0.937	2852.9	<10	<20	<10
		1.041	2748.3	<15	<20	<15
		1.081	2709.3	<15	<20	<15
		1.131	2659.0	<10	<20	<10
12	3.790	1.701	2089.5	<10	...	<10
		2.101	1689.2	76 ± 10	(76)	76 ± 10
		2.524	1266.5	4 ± 4	...	4 ± 4
		3.060	729.7	20 ± 8	<40	20 ± 8
		3.134	656.1	<10	<10	<10
		3.358	431.9	<25	<20	<20
		0	3838.5	39 ± 4	(39)	39 ± 4
		0.937	2901.4	5 ± 4	...	5 ± 4
		1.041	2796.8	<4	...	<4
		1.081	2757.8	<3	...	<3
13	3.839	1.131	2707.5	<3	<20	<3
		1.701	2138.0	4 ± 4	...	4 ± 4
		2.101	1737.7	<5	...	<5
		2.524	1315.0	<2	...	<2
		3.060	778.2	52 ± 4	(52)	52 ± 4
		3.134	704.6	<6	<11	<6
		3.358	480.4	<9	<9	<9

^a For levels 5, 7, 8, and 9 the branching ratios are the average of results from Refs. 1, 2, and 6; for level 6 they are from Refs. 1-3 and 5-7; for level 10 they are from Refs. 2 and 6; for levels 11, 12, and 13 they are from Refs. 4 and 7.

^b The branching ratios in parentheses were assumed in obtaining results for other branches.

^c A re-examination of the particle-gamma coincidence data of Ref. 6 indicates that the 3.13-MeV level branches to both the 1.04- and 1.08-MeV levels. The branching ratios extracted from these data are not inconsistent with, although much less accurate than, the present results.

distribution of the gamma rays whose peaks fall in gate B, as is illustrated by the appearance in A of the 1.04- and 1.08-MeV peaks resulting primarily from de-excitation of the 3.13-MeV level. The assignment of the weak 0.78-MeV peak in A and B to the $3.84 \rightarrow 3.06$ transition, which is known to have a 52% branching, is uncertain. To illustrate the type of information obtained from these spectra, the expected positions of a few of the possible, but unobserved transitions, are indicated in Fig. 4.

In Table IV are listed the branching ratios, or upper limits on the branching ratios, resulting from these coincidence studies. Information obtained from the singles measurements described in Sec. II A is also incorporated in this table. The summary of previous results (column 5 of Table IV) includes previously unreported upper limits on possible transitions extracted from previous work^{4,6} at this laboratory.

III. SUMMARY AND CONCLUSIONS

The information contributed by the present work is summarized in Tables II, III, and IV. Our main contribution was to confirm some weak gamma-ray branches, set more severe upper limits on others, and obtain new information concerning the decay of the F^{18} 3.13-MeV level. We now discuss this latter information in detail.

Combining the mean lifetime for the 3.13-MeV level of $(0.37_{-0.10}^{+0.15}) \times 10^{-12}$ sec (Table III) with the branching ratios of Table IV results in the partial radiative widths listed in Table V. These radiative widths correspond to the transition strengths, in Weisskopf units,¹¹ also listed in Table V. Since the parity of the 3.13-MeV level is not known, both $E1$ and $M1$ strengths are given. The $3.13 \rightarrow 0$ transition is assumed to be dipole with negligible quadrupole contribution. Actually the dipole/quadrupole mixing ratio of this transition is either $x = + (0.04 \pm 0.04)$ or $|x| > 10$.⁶ If the former is correct then the assumption of a negligible quadrupole contribution is correct. If $|x| > 10$ is correct then the partial radiative width would correspond to $E2$ and $M2$ transition strengths of 0.8 and 18 Weisskopf units,¹¹ respectively. The latter is unacceptably large for a $\Delta T = 0$ $M2$ rate in a self-conjugate nucleus,¹² and thus if the 3.13-MeV level has odd parity the $3.13 \rightarrow 0$ transition is predominantly $E1$.

Also listed in Table V are the only three known $E1$ widths for decay of bound states of F^{18} . These concern the decay of the F^{18} 1.08- and 2.10-MeV levels recently shown¹³ to have odd parity.

The results summarized in Table V give no clear-cut

¹¹ D. H. Wilkinson in *Nuclear Spectroscopy*, edited by F. Ajzenberg-Selove (Academic Press Inc., New York, 1960), Part B, pp. 862 ff.

¹² E. K. Warburton, in *Isobaric Spin in Nuclear Physics*, edited by J. D. Fox and D. Robson (Academic Press Inc., New York, 1966), pp. 90-112.

¹³ A. R. Poletti, Phys. Rev. **153**, 1108 (1967).

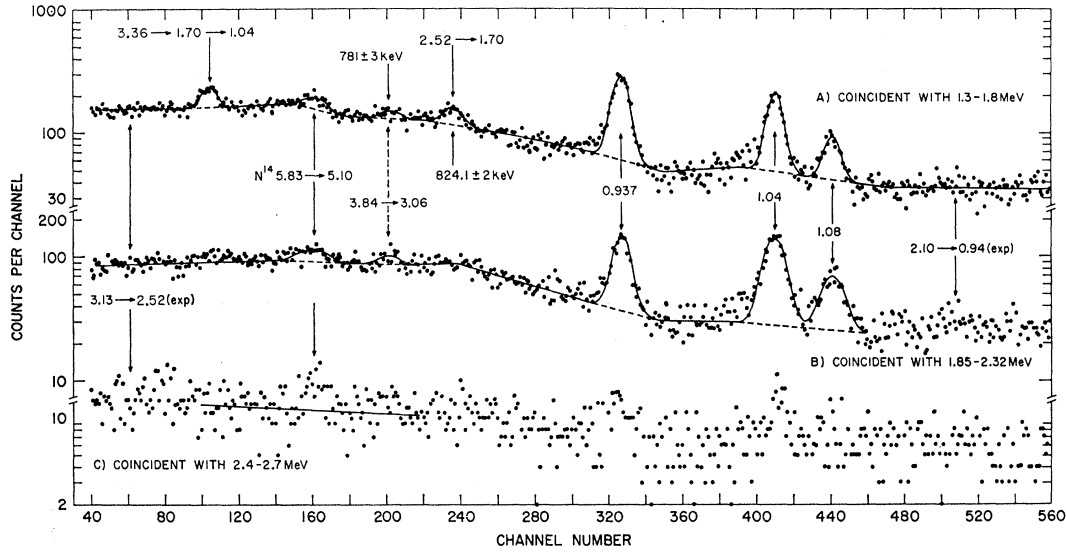


FIG. 4. Partial spectra of F^{18} gamma rays from $O^{16}+3.2\text{-MeV He}^3$ ions recorded by a 30-cc Ge(Li) detector in coincidence with pulses from a NaI(Tl) detector. The dispersion for these spectra is 1.256 keV/channel. The presence in these data of a 781 ± 3 keV peak and its assignment to the $3.84 \rightarrow 3.06$ transition is uncertain. For further details see the text and the captions of Figs. 2 and 3.

preference for either even or odd parity for the $J=1$ 3.13-MeV level.¹⁴ However, the decay modes of this level are consistent with its being the 1^- member of the odd-parity group of levels which includes the F^{18} 1.08- and 2.10-MeV levels. Such an odd-parity group of $T=0$ levels is expected in F^{18} since a group of odd-parity $T=1$ levels has been observed at higher excitation energies in both F^{18} and O^{18} . These levels probably belong predominantly to the shell-model configuration $p_{1/2}^{-1}(2s,1d)^3$ and in analogy to similar $p^{-3}(2s,1d)$ states in mass 14 and $p^{-1}(2s,1d)$ states in O^{16} , we expect these levels to be connected by $M1/E2$ transitions. Assuming $J^\pi=1^-$ for the 3.13-MeV level we see from Table V that its strongest decay mode is to the $J^\pi=0^-$ 1.08-MeV level, even though this $M1$ transition is hindered by the isotopic-spin selection rule. We also see that the

$3.13 \rightarrow 0$ transition is hindered by about the same factor as the $\Delta T=0$ $E1$ transitions from the 2.10- and 1.08-MeV levels if, in actual fact, the 3.13-MeV level has odd parity. We thus conclude that the decay of the 3.13-MeV level is consistent with its being $J^\pi=1^-$. We note that a likely candidate for the 3^- member of this group of levels is the 3.79-MeV level which decays predominantly (Table IV) to the 2.10-MeV level and has^{4,7} $J=1, 2$, or 3 .

For either parity assignment to the 3.13-MeV level, the dipole transition from it to the $T=1$ 1.04-MeV level is allowed. Thus, the extreme weakness of this dipole transition indicates a strong nuclear structure effect.

The F^{18} 3.72-MeV level has^{4,7} $J=1$ and presumably $T=0$ and decays (92%) to the $J^\pi=0^+$, $T=1$ 1.04-MeV

TABLE V. Radiative widths and transition strengths for some dipole transitions in F^{18} . (W.u. = Weisskopf units.)

Initial state E_x (MeV); J^π, T	Final state E_x (MeV); J^π, T	Γ_γ (eV)	$ M(E1) ^2$ ^a (W.u.)	$ M(M1) ^2$ ^a (W.u.)
3.13; 1,0	0; 1 ⁺ ,0	$(5.7 \pm 2) \times 10^{-4}$	4.0×10^{-5}	8.8×10^{-4}
3.13; 1,0	1.04; 0 ⁺ ,1	$(7.3 \pm 2.7) \times 10^{-4}$	1.7×10^{-4}	3.8×10^{-3}
3.13; 1,0	1.08; 0 ⁻ ,0	$(4.8 \pm 1.8) \times 10^{-4}$	1.2×10^{-4}	2.6×10^{-3}
2.10; 2 ⁻ ,0	0; 1 ⁺ ,0	$(4.6 \pm 2.2) \times 10^{-5b}$	1.1×10^{-5}	...
2.10; 2 ⁻ ,0	0.94; 3 ⁺ ,0	$(4.0 \pm 1.9) \times 10^{-5b}$	5.5×10^{-5}	...
1.08; 0 ⁻ ,0	0; 1 ⁺ ,0	$(2.2 \pm 0.2) \times 10^{-5c}$	3.7×10^{-5}	...

^a $|M|^2 = \Gamma_\gamma / \Gamma_\gamma^w$, where Γ_γ^w is the Weisskopf estimate for the radiative width (Ref. 11).

^b From Table IV and Refs. 6 (revised) and 13.

^c T. K. Alexander, K. W. Allen, and D. C. Healey, Phys. Letters 20, 402 (1966).

¹⁴ A weak preference for an odd-parity assignment to the F^{18} 3.13-MeV level is provided by the $F^{18}(\text{He}^3, \alpha)F^{18}$ angular-distribution measurements of G. M. Matous, G. H. Herling, and E. A. Wolicki, Bull. Am. Phys. Soc. 11, 333 (1966); Phys. Rev. 152, 908 (1966).

level (Table IV). Thus the upper limit to the mean lifetime of this level (Table III) is consistent with expectations for this isotopic-spin-allowed dipole transition.

ACKNOWLEDGMENTS

We would like to thank Professor A. Gallmann and Dr. R. M. Freeman for helpful discussions and communications.

$^{14}\text{N}(^3\text{He},t)^{14}\text{O}$ Reaction and Excited Isospin Triads in Mass 14*

GORDON C. BALL AND JOSEPH CERNY

Department of Chemistry and Lawrence Radiation Laboratory, University of California, Berkeley, California

(Received 3 November 1966)

The $^{14}\text{N}(^3\text{He},t)^{14}\text{O}$ reaction has been investigated at a ^3He energy of 44.6 MeV. New levels were observed in ^{14}O up to an excitation energy of 18 MeV. An investigation of the $(^3\text{He},t)$ reaction on several other nuclei in the $1p$ shell, notably ^{14}C and ^{15}N , revealed that the shapes and relative magnitudes of the angular distributions arising from single-particle transitions appear to fall into groups which are characterized by the specific shell-model transition involved. Utilizing this effect and other data, it was possible to make most probable spin and parity assignments of $(1-)$, $(0+)$, $(3-)$, $2+$, $(2-)$, and $2+$ for the levels observed in ^{14}O at 5.17, 5.91, 6.28, 6.60, 6.79, and 7.78 MeV, respectively. A correspondence can now be established for six excited $T=1$ levels in all three members of the mass-14 triad.

I. INTRODUCTION

VARIOUS theoretical treatments have been able to predict with reasonable accuracy the Coulomb energy differences observed in ground isobaric multiplets of $T \leq 1$ nuclei, particularly in the $1p$ shell.¹⁻³ As a result, a charge dependence of nuclear forces of $\leq 2\%$ can be estimated.² Coulomb energy differences have also been calculated for excited states in $1p$ -shell mirror nuclei³ and satisfactory agreement is obtained if other effects such as the Thomas-Ehrman shift⁴ are taken into account. It would clearly be useful to know the results of similar calculations on other excited isobaric multiplets; however, very little experimental evidence exists for complete correspondences among excited states in isobaric multiplets of $T > \frac{1}{2}$.

The mass-14 triad is an especially attractive system to investigate since more is known about the $T=1$ levels of ^{14}N than of any other $T_z=0$ nucleus. In addition, the energy levels of ^{14}C have been extensively studied. All that is necessary to complete this triad is a knowledge of the levels of ^{14}O , which can be investigated through the $^{14}\text{N}(^3\text{He},t)^{14}\text{O}$ reaction. We have found

that the angular distributions observed in the $(^3\text{He},t)$ reaction on several light nuclei have characteristic shapes which depend on the nature of the single-particle transitions involved. By exploiting this effect in conjunction with other available data, it has been possible to assign most probable spins and parities to the levels observed in ^{14}O below 8 MeV. In this manner a correspondence has been established for six excited $T=1$ levels in all three members of the mass-14 triad.

II. EXPERIMENTAL

The $^{14}\text{N}(^3\text{He},t)^{14}\text{O}$ reaction was carried out at an energy of 44.6 MeV using a ^3He beam from the Berkeley 88-in. cyclotron. Particles were detected using a $(dE/dx-E)$ counter telescope which fed a particle identifier⁵; complete separation was obtained between tritons and deuterons. The (dE/dx) counter was a 300- μ phosphorus-diffused silicon detector while the E counter consisted of a 3-mm lithium-drifted silicon detector which was rotated 30° in order to stop the high-energy tritons. A more detailed discussion of the experimental equipment will be presented elsewhere.⁶

Both a N_2 gas target and a solid adenine ($\text{C}_5\text{H}_5\text{N}_5$) target were used. The gas was contained in a 7.66-cm diameter cell with a window of Havar⁷ foil 0.00025 cm thick. The solid target was made by evaporating ≈ 1.1 mg/cm² of adenine onto a 150 $\mu\text{g}/\text{cm}^2$ carbon backing. No detectable decomposition of the target was observed over a period of 48 h at beam intensities of 100–400 nA.

* Work performed under the auspices of the U. S. Atomic Energy Commission.

¹ B. C. Carlson and I. Talmi, *Phys. Rev.* **96**, 436 (1954); S. Sengupta, *Nucl. Phys.* **21**, 542 (1960); W. M. Fairbairn, *Proc. Phys. Soc. (London)* **77**, 599 (1961); L. Lovitch, *Nucl. Phys.* **46**, 353 (1963); **53**, 477 (1964); R. J. Blin-Stoyle and S. C. K. Nair, *Phys. Letters* **7**, 161 (1963); R. J. Blin-Stoyle, *Selected Topics in Nuclear Spectroscopy* (North-Holland Publishing Company, Amsterdam, 1964), p. 213; R. J. Blin-Stoyle and C. Yalgin, *Phys. Letters* **15**, 258 (1965).

² D. H. Wilkinson, *Phys. Rev. Letters* **13**, 571 (1964); D. H. Wilkinson and W. D. Hay, *Phys. Letters* **21**, 80 (1966).

³ W. M. Fairbairn, *Nucl. Phys.* **45**, 437 (1963).

⁴ R. G. Thomas, *Phys. Rev.* **81**, 148 (1951); **88**, 1109 (1952); J. B. Ehrman, *ibid.* **81**, 412 (1951).

⁵ F. S. Goulding, D. A. Landis, J. Cerny, and R. H. Pehl, *Nucl. Instr. Methods* **31**, 1 (1964).

⁶ D. G. Fleming, C. C. Maples, and J. Cerny (to be published).

⁷ Hamilton Watch Company, Waltham, Massachusetts.